Published Online: 2026 April 21 **Research Article**

Glycyrrhetinic Acid Inhibits Malignant Progression of Hepatocellular Carcinoma by Inducing Autophagy and Regulating Macrophage Polarization via the TGF-β1/SMAD Pathway

Youjin Wang [#1], Huiyun Guan [#2], Peibei Duan [3,*]

[1] Department of Radiology, Jiangsu Province Hospital of Chinese Medicine, Affiliated Hospital of Nanjing University of Chinese Medicine, Nanjing, China
[2] School of Nursing, Nanjing University of Chinese Medicine, Nanjing, China
[3] Department of Nursing, Affiliated Hospital of Nanjing University of Chinese Medicine, Nanjing, China

[*] ***Corresponding Author:*** Affiliated Hospital of Nanjing University of Chinese Medicine, Nanjing, China. Email: dpb_5889@hotmail.com
# These authors have contributed equally

Received: 13 December, 2025; **Revised:** 14 January, 2026; **Accepted:** 7 February, 2026

Abstract

Background: Hepatocellular carcinoma (HCC) is one of the most aggressive malignancies, and its poor prognosis is primarily attributed to its complex tumor microenvironment (TME). Glycyrrhetinic acid (GA) possesses potent anti-tumor properties, but its mechanisms of action and molecular targets within the HCC microenvironment remain to be thoroughly explored. Methods:

Methods: This study employed HCC cell lines and a mouse xenograft model. In vitro experiments, we evaluated the effects of GA on HCC cell proliferation, migration, invasion, and apoptosis, and analyzed its role in M2 macrophage polarization within a co-culture system. Interventions using the autophagy inhibitor chloroquine (CQ) and the TGF-β1 signaling pathway activator SRI-011381 were performed, and the expression levels of autophagy markers, M1/M2 macrophage markers, and TGF-β1/SMAD pathway-related proteins were detected. In vivo experiments, we assessed the effects of GA on tumor progression, autophagy processes, and M2 macrophage infiltration.

Results: In vitro, GA significantly inhibited malignant behaviors of HCC cells and promoted their apoptosis and autophagy. Furthermore, GA treatment effectively blocked M2 macrophage polarization and their pro-tumorigenic function in the co-culture system, an effect that was significantly reversed by CQ. Regarding the molecular mechanism, GA was found to inhibit the activation of the TGF-β1/SMAD axis, and the TGF-β1 pathway activator SRI-011381 reversed GA's induction of autophagy and inhibition of M2 polarization. In animal experiments, GA treatment significantly suppressed tumor growth and promoted cell apoptosis; concurrently, GA promoted autophagy and reduced M2 macrophage infiltration in tumor tissues. All these effects were reversible by SRI-011381.

Conclusions: Glycyrrhetinic acid inhibits HCC malignant progression by suppressing the TGF-β1/SMAD axis, inducing autophagy in HCC cells, and inhibiting M2 macrophage polarization

Keywords: Glycyrrhetinic Acid, Hepatocellular Carcinoma, Macrophage Polarization, TGF-β1/SMAD, Autophagy

1. Background

Hepatocellular carcinoma (HCC) is a highly aggressive malignancy with a global presence, posing a significant public health burden due to its high incidence and unfavorable survival rates (1-3). Current treatment strategies for advanced HCC have limited efficacy, with tumor drug resistance, recurrence, and metastasis remaining major obstacles in clinical practice (4, 5). The tumor microenvironment (TME), an essential local niche for neoplastic sustenance, is a well-established determinant of carcinogenesis, tumor evolution, and therapy efficacy (6). Tumor-associated macrophages (TAMs), which are the predominant infiltrating immune population within the cellular and non-cellular matrix of the TME, play a central role in facilitating HCC initiation, progression, and immune evasion (7, 8). However, despite their recognized

How to Cite: Wang Y, Guan H, Duan P. Glycyrrhetinic Acid Inhibits Malignant Progression of Hepatocellular Carcinoma by Inducing Autophagy and Regulating Macrophage Polarization via the TGF-β1/SMAD Pathway. Hepat Mon. 2026;26(1):e169009. doi: https://doi.org/10.5812/hepatmon-169009

importance, effective strategies to clinically reprogram pro-tumorigenic M2 macrophages into anti-tumor M1 phenotypes remain elusive, representing a significant gap in HCC immunotherapy. Tumor-associated macrophages exhibit remarkable functional plasticity, shifting between anti-tumor (M1) and pro-tumorigenic (M2) phenotypes in response to microenvironmental cues (9). In HCC, the abundance of M2 macrophages creates an immunosuppressive milieu that supports angiogenesis and tissue remodeling (10, 11). Conversely, M1 macrophages are associated with pro-inflammatory, anti-tumor responses (12, 13). Consequently, reprogramming TAMs from an M2 to an M1 phenotype has emerged as a promising strategy for HCC immunotherapy. The orchestration of macrophage polarization involves an intricate network of signaling pathways and homeostatic processes, among which autophagy and the transforming growth factor-beta 1 (TGF-β1) signaling axis are of particular interest (14-16). TGF-β1 acts as a potent driver of M2 polarization and TME immunosuppression (17). As an overexpressed and potent immunosuppressive factor in the HCC microenvironment, TGF-β1 is well established as a pivotal driver of M2 macrophage polarization (18). Emerging evidence suggests a potential crosstalk in which the TGF-β1 pathway modulates autophagy to foster a tumor-favorable environment (19). Thus, identifying agents that can precisely intervene in this TGF-β1/autophagy axis represents a focal point of current HCC research. Currently, identifying drug molecules capable of precisely intervening in this regulatory axis has become a research focus. Glycyrrhetinic acid (GA) exhibits pleiotropic biological effects, encompassing anti-inflammatory, hepatoprotective, and anti-tumor functions (20). Its anti-tumor mechanisms extend beyond direct cytotoxicity to include systemic regulation of the TME. Studies have shown that GA can influence macrophage phenotype and inhibit tumor cell migration in breast cancer models (21). Furthermore, GA can regulate cellular autophagy activity under various pathological conditions (22, 23).

2. Objectives

The present study aimed to investigate whether GA could inhibit HCC malignant progression by modulating the TGF-β1/SMAD axis and its downstream effects on autophagy and macrophage polarization. Our findings provide a novel immunometabolic explanation for GA's anti-tumor activity and offer potential molecular targets for HCC immunotherapy (Figure 1).

3. Methods

3.1. Cell Culture and Induction

The HCC cell lines (Li-7, STCC10107G; HuH-7, STCC10102P; HCC-LM3, STCC10111P; Hepa1-6, STCC00016P) were all purchased from Servicebio (Wuhan, China). The human monocytic cell line THP-1 (CL-0233) and the normal human hepatocyte cell line THLE-2 (CL-0833) were procured from Procell Life Science & Technology Co., Ltd. (Wuhan, China). For culture media selection, Li-7 and THP-1 cells were maintained in RPMI 1640 medium (11875093, Gibco, Grand Island, NY, USA) supplemented with 10% FBS (G8003, Servicebio) and 1% penicillin-streptomycin (P/S, PB180120, Procell, Connecticut, USA), while HuH-7, HCC-LM3, THLE-2, and Hepa1-6 cells were cultured in DMEM medium (11965092, Gibco) supplemented with 10% FBS and 1% P/S. To obtain macrophages with different polarization states, THP-1 monocytes were first treated with 100 ng/mL phorbol 12-myristate 13-acetate (PMA, HY-18739, MCE, Monmouth Junction, NJ, USA) for 24 h to induce differentiation into M0 macrophages. Subsequently, M0 macrophages were induced to polarize into M1 or M2 phenotypes. M1 macrophages were induced by co-incubation with lipopolysaccharide (LPS, 100 ng/mL, SMB00610, Sigma, St. Louis, MO, USA) and interferon-γ (IFN-γ, 10 ng/mL, SRP3058, Sigma) (24). M2 macrophages were obtained by co-treatment with interleukin-4 (IL-4, 20 ng/mL, 200-04, Gibco) and IL-13 (20 ng/mL, 200-13, Gibco) (25). Successful induction was confirmed by flow cytometry detection of specific surface markers.

3.2. Cell Treatment

To thoroughly investigate the effects of GA on HCC (Li-7, HuH-7) and macrophages, as well as its underlying mechanisms, this study designed three distinct cell treatment protocols. Glycyrrhetinic acid (purity > 99%; HY-N0180, MCE) was dissolved in dimethyl sulfoxide (DMSO, ST038, Beyotime, Shanghai, China) to prepare a stock solution. First, to determine the effective working concentration of GA, cells were treated with GA (0/50/100/150 μM) for 24 h. Second, to investigate the involvement of autophagy in GA-mediated effects, the cells were allocated into three groups: Control, 150 μM GA, and 150 μM GA + 10 μM chloroquine (CQ, an autophagy inhibitor, HY-17589A, MCE). For this experimental design, a 1-hour pretreatment with 10 μM CQ was applied, after which cells were co-incubated with 150 μM GA for 24 hours. To further probe the role of the TGF-β1/SMAD pathway in GA-mediated autophagy and macrophage polarization, an additional set of cells was assigned to three groups: Control, 150 μM GA, and 150 μM GA combined with 10 μM SRI-011381 (a TGF-β1

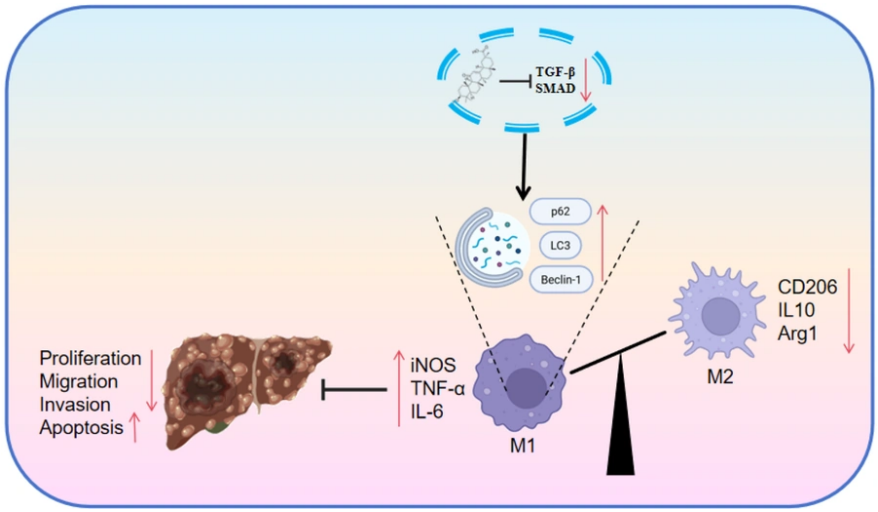

Figure 1. Glycyrrhetinic acid induces autophagy by inhibiting the TGF-β1/SMAD signaling pathway, thereby promoting anti-tumor macrophage polarization and ultimately suppressing the malignant progression of hepatocellular carcinoma.

signaling activator; Selleck Chemicals, USA). In this regimen, cells received a 1-hour pretreatment with 10 μM SRI-011381 prior to a 24-hour co-treatment with 150 μM GA.

3.3. Animals and Treatment

For the in vivo validation of GA's inhibitory effect on HCC progression and the associated mechanisms, establishment of a mouse HCC xenograft model was undertaken in this investigation. C57BL/6 mice (6-8 weeks old) were purchased from Shanghai SLAC Laboratory Animal Co., Ltd. All animal experiments were approved by the Affiliated Hospital of Nanjing University of Chinese Medicine Ethics Committee. Establishment of the HCC subcutaneous xenograft model was performed according to a previous method (26), involving the injection of Hepa1-6 cells (5×10^6 cells in PBS) into the right inguinal fold. Randomization of mice into four experimental groups (9 mice per group) was carried out when tumor volumes attained 100 mm^3. The groups were designated as follows: Control (daily i.p. 0.9% saline), GA low-dose (25 mg/kg GA daily i.p.), GA high-dose (50 mg/kg GA daily i.p.), and GA + SRI-011381 (50 mg/kg GA and 30 mg/kg SRI-011381 daily i.p.). Administration of treatments continued for a duration of 4 weeks, with weekly measurement of tumor volumes. After the experiments, mice were euthanized for subsequent histological and molecular biological analyses, and tumor, liver, and kidney tissues were harvested. Tumor tissues were weighed and photographed, with a portion immediately stored in liquid nitrogen. Other portions of tumor tissue, along with liver and kidney tissues, were used for histological and immunohistochemical analysis. Tumor tissues were dissociated using a commercial tumor dissociation kit (abs50090, Absin, Shanghai, China). Filtration of the dissociated tissue suspension was performed through a 70 μm cell strainer (CLS431751, Sigma) for the removal of tissue clumps, followed by further purification via 36% Percoll gradient centrifugation (BS909, Biosharp, Hefei, China) to obtain high-quality single-cell suspensions for subsequent flow cytometry analysis. Additionally, femurs and tibias were extracted from mice to isolate bone marrow cells, which were then cultured for 7 days in DMEM medium supplemented with 10% FBS, 1% P/S, and 40 ng/mL macrophage colony-stimulating factor (M-CSF, 315-02, Gibco) to induce differentiation into bone marrow-derived macrophages (BMDMs).

3.4. Cell Co-culture

To simulate HCC cell-macrophage interactions within the TME, Transwell inserts (0.4 μm pore size) were used in two configurations: M2-polarized THP-1 macrophages were seeded in the upper chamber, with Li-7 or HuH-7 cells (5×10^5) in the lower chamber. BMDMs were placed in the lower chamber and Hepa1-6 cells in the upper chamber (27). Both systems were co-cultured for 48 h prior to further experimentation.

3.5. Cell Counting Kit-8 Assay

Cell viability following GA treatment was determined by cell counting kit-8 assay (CCK-8, A311-01, Vazyme). Cells were plated at 3×10^3/well and treated with GA (0, 12.5, 25, 50, 100, 150, 200 μM) for 24 h or 48 h. After adding CCK-8 solution (10 μL/well) and incubating for 3 h at 37°C, absorbance was read at 450 nm for viability calculation.

3.6. mRFP-GFP-LC3B Viral Transfection

Autophagic flux was assessed using the mRFP-GFP-LC3 tandem reporter lentivirus (Hanbio, Shanghai, China). Hepatocellular carcinoma cells (2×10^4/well) were infected at an MOI of 20 with 5 μg/mL polybrene (S2667, Sigma). After 24 h, the medium was changed and cells were treated as indicated for another 24 h. Following fixation and mounting with DAPI-containing medium (P0133, Beyotime), cells were imaged on a confocal microscope (SP8, Leica, Wetzlar, Germany). Autophagosomes (yellow) and autolysosomes (orange-red) were distinguished based on GFP/mRFP colocalization.

3.7. EdU Staining

Proliferation was measured by EdU incorporation (abs50053, Absin). GA-treated HCC cells in 96-well plates were incubated with 10 μM EdU for 2 h. After standard fixation/permeabilization and a 30-min dark incubation for fluorescent detection, nuclei were stained with Hoechst 33342 (C1025, Beyotime). EdU-positive cells were counted from fluorescence images.

3.8. Scratch Assay

A scratch assay was used to measure migration. Li-7 and HuH-7 cells (5×10^5/well in 6-well plates) were treated as indicated. A scratch was made with a pipette tip, and after washing, wound areas were imaged at 0 h and 24 h post-scratch using a microscope (CKX 53, OLYMPUS, Tokyo, Japan). Cell migration rates were quantitatively analyzed and calculated using ImageJ software.

3.9. Transwell Assay

Cell invasion was measured using Matrigel-coated Transwell chambers. Treated Li-7/HuH-7 cells (2×10^4/well) in Opti-MEM (11058021, Gibco) containing GA were seeded in the upper chamber, with 10% FBS medium in the lower chamber as a chemoattractant. After 24 h, non-invading cells were removed, and invaded cells on the lower membrane were fixed, stained (0.1% crystal violet, V5265, Sigma), and counted in five fields/membrane.

3.10. Immunofluorescence

Analysis of TGF-β1 expression and localization was performed via immunofluorescence. Following seeding into 6-well plates and GA treatment, Li-7 and HuH-7 cells underwent fixation with 4% PFA and permeabilization with 0.1% Triton X-100. Blocking was achieved using 5% BSA (PB180642, Procell). Incubation with a TGF-β1 primary antibody (GTX45121, GeneTex, Irvine, CA, USA) was carried out overnight at 4°C. After washing, treatment with a fluorescent secondary antibody (GTX213110-04, GeneTex) was conducted for 1 h at room temperature. Staining of nuclei was performed with DAPI (BL105A, Biosharp) for 5 min. Finally, image acquisition was performed with a confocal fluorescence microscope.

3.11. Immunohistochemistry

Ki67 immunohistochemistry was performed on xenograft tumor sections to assess GA's effect on proliferation. Sections (4 μm) were processed through standard dewaxing, rehydration, and antigen retrieval in citrate buffer (pH 6.0, C492977, Aladdin, Shanghai, China). After peroxidase blocking (3% H_2O_2, 7722-84-1, Aladdin), staining was performed with anti-Ki67 (1:500, 27309-1-AP, Proteintech, Wuhan, China) overnight at 4°C, followed by HRP-secondary antibody (GTX213110-01, GeneTex) and DAB development (P0202, Beyotime). Hematoxylin (517-28-2, Aladdin) was used for counterstaining. Ki67-positive cells were quantified from microscope images.

3.12. Terminal Deoxynucleotidyl Transferase dUTP Nick End Labeling Staining

Apoptosis within tumor tissues was detected via terminal deoxynucleotidyl transferase dUTP nick end labeling staining using a commercial kit (T2130, Solarbio, Beijing, China). Deparaffinized and rehydrated paraffin sections were subjected to proteinase K digestion (P1120, Solarbio) for 15 min. Following PBS washes, the sections were incubated with the terminal deoxynucleotidyl transferase dUTP nick end labeling reaction mixture at 37°C in a humidified chamber for 1 h. After another wash, nuclei were counterstained with DAPI. Fluorescence images were captured from five random fields per section, and the apoptosis rate was quantified as the percentage of terminal

deoxynucleotidyl transferase dUTP nick end labeling-positive cells.

3.13. Hematoxylin and Eosin Staining

Liver and kidney tissues from the mouse xenograft tumor model were collected, fixed with 4% PFA, and paraffin-embedded. After deparaffinization and rehydration, sections were stained using a hematoxylin and eosin kit (HE, G1120, Solarbio), undergoing hematoxylin staining, differentiation, bluing, and eosin staining sequentially. Finally, sections were dehydrated, cleared, mounted with neutral balsam (BL704A, Biosharp), and observed under a microscope.

3.14. Enzyme-Linked Immunosorbent Assay

Supernatants were collected from co-cultured M2 macrophages subjected to various treatment conditions. Human or mouse IL-10 (88-7106-88; 88-7105-22, Invitrogen, Carlsbad, CA, USA) and TGF-β1 (SEKH-0316; SEKM-0035, Solarbio) were then analyzed. According to the kit instructions, samples and standards were added to antibody-coated 96-well plates. After sequential incubations and washes with detection antibody and HRP-streptavidin, color was developed using substrate (dark incubation). The reaction was stopped, and absorbance at 450 nm was read on a microplate reader.

3.15. Flow Cytometry

To detect apoptosis, GA-treated Li-7 and HuH-7 cells (1×10^7 cells/mL) were collected, stained using an Annexin V-FITC/PI apoptosis detection kit (HY-K1073, MCE), and analyzed by flow cytometry to calculate the apoptosis rate. To analyze macrophage phenotypes, THP-1 cells were collected and stained with the following fluorescently labeled antibodies: for M0, FITC-CD14 (11-0149-41, Invitrogen) and APC-CD11b (CD11B05, Invitrogen) antibodies were added and incubated on ice for 1 h; for M1, PE-CD86 (MHCD8604, Invitrogen) and APC-CD11b (CD11B05, Invitrogen) antibodies were added and incubated on ice for 1 h; for M2, FITC-CD206 (MA562234, Invitrogen) and APC-CD11b (CD11B05, Invitrogen) antibodies were added and incubated on ice for 1 h. For GA-treated M1/M2 macrophages, cells were stained with PE-CD86 (MHCD8604, Invitrogen) or FITC-CD206 (MA562234, Invitrogen), respectively, to analyze the effect of GA on M1 or M2 macrophage phenotypes. Single-cell suspensions prepared from mouse tumor tissues were incubated with CD16/32 antibody (MFCR00-4, Invitrogen) for 15 min at 4°C to reduce non-specific binding. Subsequently, cells were stained in the dark for 30 min with PerCP-CD45 (MHCD4530, Invitrogen), APC-CD11b (17-0112-83, Invitrogen), PE-Cy7-F4/80 (25-4801-82, Invitrogen), and FITC-CD206 (MA5-16870, Invitrogen), respectively. Flow cytometry was used to analyze the proportion of F4/80-positive macrophages within the CD45-positive cell population, and the proportion of CD206-positive M2-type cells within this macrophage population. Additionally, the proportion of M2-type cells in BMDMs co-cultured with Hepa1-6 cells was detected by flow cytometry using PE-CD206 antibody (12-2061-82, Invitrogen) staining.

3.16. Western Blot

Total proteins were extracted from mouse tumor tissues and cells using RIPA lysis buffer (P0013C, Beyotime) containing protease/phosphatase inhibitors. Protein concentrations were determined using a BCA protein assay kit (P0012, Beyotime). Equal amounts of protein (20 - 40 μg) were separated by SDS-PAGE and transferred to PVDF membranes. Membranes were blocked with 5% BSA for 1 h and then incubated overnight at 4°C with the following primary antibodies: iNOS (1:100, ab178945, Abcam, Cambridge, MA, USA), TNF-α (1:1000, #3707, CST, Danvers, MA, USA), IL-6 (1:1000, #12153, CST), CD206 (1:1000, #24595, CST), IL-10 (1:2000, GTX130513, GeneTex), Arg1 (1:200, ab124917, Abcam), LC3 (1:2000, 14600-1-AP, Proteintech), sequestosome 1 (p62, 1:8000, 84826-1-RR, Proteintech), Beclin1 (1:5000, Proteintech, 11306-1-AP), TGF-β1 (1:1000, #3711, CST), p-SMAD2 (1:500, GT1291, GeneTex), SMAD2 (1:500, GTX111075, GeneTex), p-SMAD3 (1:500, GTX00969, GeneTex), SMAD3 (1:2000, GTX34208, GeneTex), and GAPDH (1:1000, #2118, CST). After incubation with appropriate HRP-conjugated secondary antibodies (1:10000, GTX213110-01/GTX213111-01, GeneTex) for 1 h, signals were developed using an ECL chemiluminescence kit (P0018, Beyotime). Grayscale analysis was performed using ImageJ software, with GAPDH serving as an internal control.

3.17. Statistical Analysis

Data are presented as mean ± standard deviation (SD). Statistical analyses were performed using GraphPad Prism software. The Shapiro-Wilk test was used to determine whether data followed a normal distribution before conducting parametric or non-parametric tests. When data met normal distribution and had equal variances, differences in means were analyzed using Student's *t*-test or one-way ANOVA; otherwise, non-parametric test methods (Wilcoxon test) were employed. A P-value less than 0.05 was considered statistically significant.

4. Results

4.1. Glycyrrhetinic Acid Inhibits Proliferation, Migration, Invasion, and Promotes Apoptosis of HCC Cells

Initially, we investigated whether GA possesses direct anti-tumor properties against HCC cell lines. To evaluate the impact of GA (chemical structure shown in Figure 2A) on HCC progression, we first assessed its effect on cell viability. While GA concentrations up to 200 μM were required to impair the viability of human normal THLE-2 hepatocytes, Li-7, HuH-7, and HCC-LM3 cells displayed high sensitivity to GA treatment, with significant growth inhibition observed at doses of 50, 100, and 150 μM (Figure 2B-E). Consequently, Li-7 and HuH-7 cells were selected for subsequent experiments involving a 24 h exposure to these concentrations. The multifaceted anti-tumor activity of GA was further evidenced by a marked reduction in DNA synthesis, as indicated by decreased EdU incorporation (Figure 2F-H). Beyond growth suppression, GA treatment effectively curtailed the metastatic potential of HCC cells. Specifically, both scratch assays and Matrigel-coated Transwell assays demonstrated a substantial, dose-dependent decline in migratory and invasive capacities (Figure 2I-N). Furthermore, flow cytometric analysis confirmed that these anti-proliferative effects were accompanied by a significant induction of apoptosis (Figure 2O-Q), which underscores the potent pro-apoptotic properties of GA.

4.2. Glycyrrhetinic Acid Inhibits pro-tumorigenic Polarization of Tumor-Associated Macrophages, Thereby Suppressing Hepatocellular Carcinoma Cell Viability and Promoting Apoptosis

Beyond its direct effects on tumor cells, the therapeutic potential of GA may also involve modulation of the immunosuppressive TME, particularly the polarization of TAMs. The polarization status of TAMs within the TME is a critical determinant of tumor fate. After successfully differentiating THP-1 cells into M0, M1, and M2 phenotypes with induction efficiencies exceeding 90% (Figure 3A-C), we investigated the immunomodulatory role of GA. Western blot analysis of M1 and M2 marker proteins showed that GA upregulated iNOS, TNF-α, and IL-6 expression in M1 macrophages, while it inhibited CD206, IL-10, and Arg1 expression in M2 macrophages (Figure 3D-K). Flow cytometry analysis further confirmed that GA significantly increased the number of CD86+ cells in M1 macrophages and reduced the proportion of CD206+ cells in M2 macrophages (Figure 3L-O). These findings imply that GA, by regulating macrophage phenotypic polarization, promotes inflammatory responses and suppresses the immunosuppressive microenvironment. To further explore whether these immunomodulatory effects translated into anti-cancer benefits, a co-culture system simulating the HCC microenvironment was utilized (Figure 3P). Enzyme-linked immunosorbent assay results demonstrated that GA significantly reduced the secretion of M2-associated pro-tumorigenic cytokines, such as IL-10 and TGF-β1, into the culture supernatant (Figure 3Q-R). Most importantly, the presence of GA effectively abrogated the ability of M2 macrophages to promote HCC cell proliferation, migration, and invasion, while simultaneously sensitizing these cells to apoptosis (Figure 3S-Z). Collectively, these findings suggest that GA inhibits HCC progression by interfering with the pro-tumorigenic crosstalk mediated by M2-polarized macrophages.

4.3. Glycyrrhetinic Acid Induces Autophagy in Hepatocellular Carcinoma Cells, Thereby Interfering with Pro-tumorigenic Polarization of Tumor-Associated Macrophages

Considering that GA-treated HCC cells exhibited a reduced capacity to stimulate M2 polarization, we next explored whether GA triggers specific intracellular processes, such as autophagy, which is often involved in cancer-cell-mediated immune modulation. To investigate whether GA's inhibition of HCC cell malignant progression is related to autophagy, we tested GA's effect on autophagy markers in HCC cells via Western blot. Results showed that GA dose-dependently increased the LC3-II/LC3-I ratio and enhanced the expression of p62 and Beclin1, suggesting that GA can induce autophagy in HCC cells (Figure 4A-C). Subsequently, autophagic flux was further validated using the mRFP-GFP-LC3B tandem fluorescent reporter virus transfection assay. Results indicated that after treatment with 150 μM GA, the numbers of both GFP-LC3 and mRFP-LC3 fluorescent puncta within cells were significantly increased (Figure 4D-F), demonstrating that GA not only promotes autophagosome formation but also enhances autophagic flux. To explore the role of GA-mediated autophagy in M2 polarization, we employed a combined intervention with CQ (an autophagy inhibitor) and GA. Co-treatment with CQ and GA led to a reduction in both GFP-LC3 and mRFP-LC3 puncta, indicating that CQ inhibits GA-induced autophagy. Notably, CQ treatment markedly antagonized the suppressive effect of 150 μM GA on HCC cell viability (Figure 4G-H). In the HCC/M2 macrophage co-culture system, the combination of GA and CQ resulted in significantly elevated levels of IL-10 and TGF-β1 in the supernatant, along with increased expression of M2 marker proteins, compared to GA treatment alone (Figure 4I-N). These collective findings suggest that GA

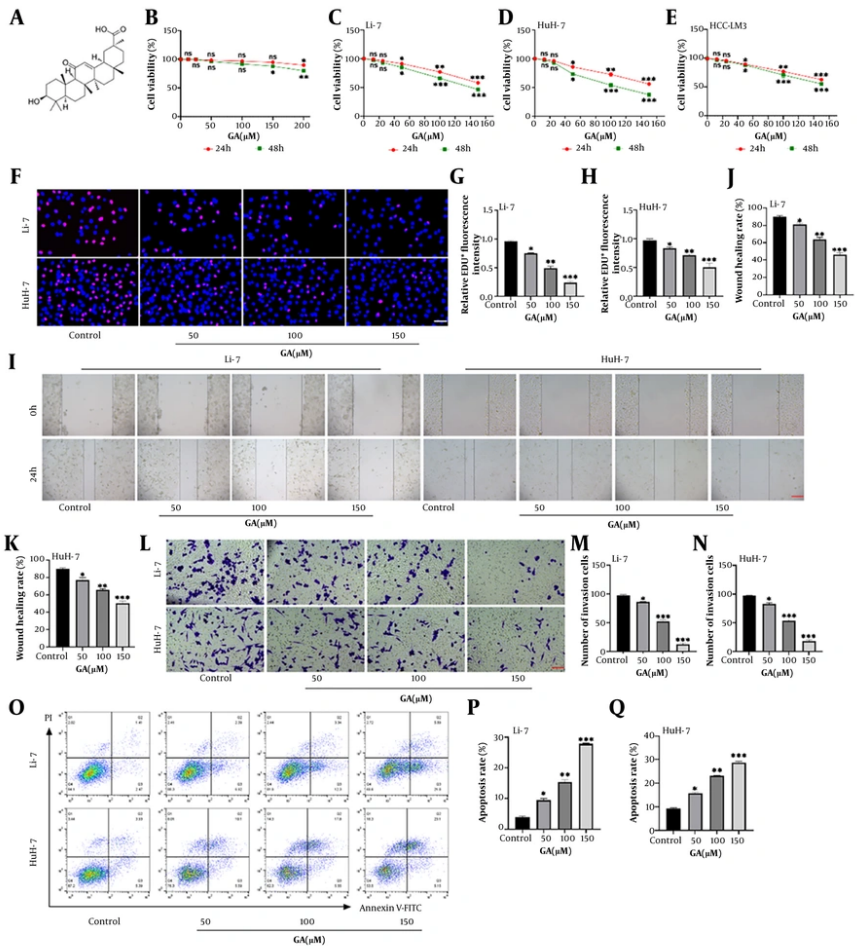

Figure 2. Glycyrrhetinic acid (GA) inhibits the proliferation, migration, and invasion of hepatocellular carcinoma (HCC) cells while promoting apoptosis. A, chemical structure of GA; B, effect of different concentrations of GA (0/12.5/25/50/100/150/200 μM) on the viability of human normal hepatocyte THLE-2 cells after 24 h treatment, as determined by cell counting kit-8 (CCK-8) assay; C-E, effect of different concentrations of GA (0/12.5/25/50/100/150 μM) on the viability of Li-7, HuH-7, and HCC-LM3 after 24 h and 48 h treatment, respectively, as determined by CCK-8 assay; F-H, effect of GA treatment for 24 h on the proliferation of HCC cells, analyzed by EdU staining (scale bar: 50 μm); I-K, effect of GA treatment for 24 h on the migration of HCC cells, determined by scratch assay (scale bar: 200 μm); L-N, effect of GA treatment for 24 h on the invasion of HCC cells, analyzed by Transwell invasion assay (scale bar: 100 μm); O-Q, effect of GA treatment for 24 h on the apoptosis of HCC cells, detected by flow cytometry (ns: $P > 0.05$, * $P < 0.05$, ** $P < 0.01$, *** $P < 0.001$ vs control).

disrupts tumor-associated macrophage M2 polarization by inducing autophagy in HCC cells.

4.4. GA Inhibits the TGF-β1/SMAD Pathway

Having established the importance of autophagy in GA-mediated effects, we turned our attention to the upstream signaling pathways, specifically the TGF-β1/SMAD axis, which is a well-known regulator of both autophagy and the tumor immune landscape (28). To elucidate the mechanisms underlying GA-induced autophagy and macrophage modulation, we investigated its impact on the TGF-β1/SMAD signaling axis. Glycyrrhetinic acid treatment elicited a dose-dependent downregulation of TGF-β1 expression and marked suppression of SMAD2/3 phosphorylation in HCC cells, while total SMAD2/3 protein levels remained stable (Figure 5A-D). These observations were further corroborated by immunofluorescence assays, which showed that GA significantly reduced the fluorescence intensity of TGF-β1 in both HCC cell lines (Figure 5E-F). Collectively, these data indicate that GA acts by attenuating the TGF-β1/SMAD signaling pathway.

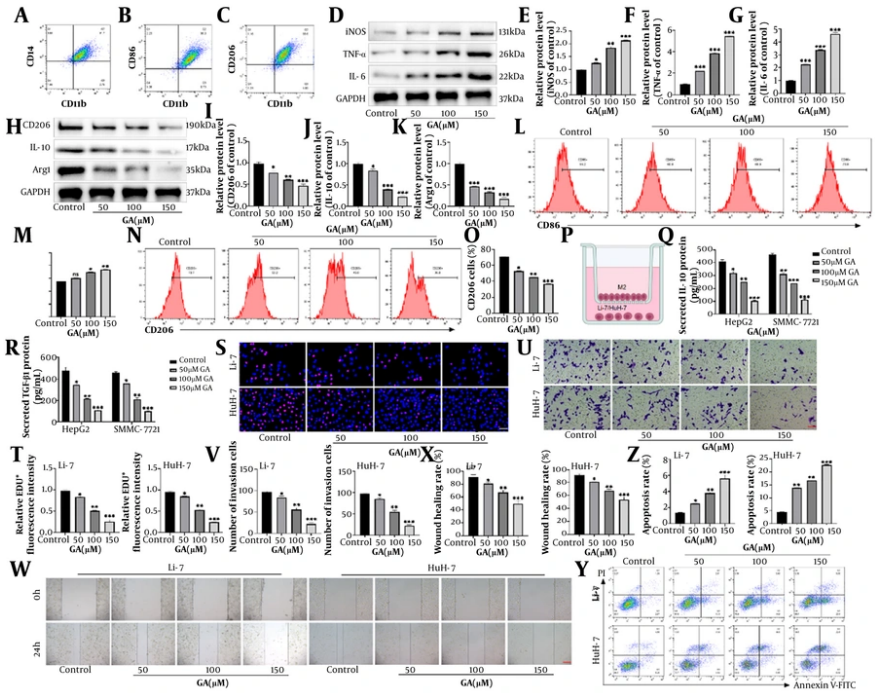

Figure 3. Glycyrrhetinic acid inhibits M2 polarization of TAMs, thereby suppressing HCC cell viability and promoting apoptosis. A, identification of successful differentiation of THP-1 cells into M0 macrophages by detecting CD11b and CD14 expression via flow cytometry; B, identification of successful differentiation of THP-1 cells into M1 macrophages by detecting CD11b and CD86 expression via flow cytometry; C, identification of successful differentiation of THP-1 cells into M2 macrophages by detecting CD11b and CD206 expression via flow cytometry; D-G, western blot analysis of the effect of GA on M1 marker protein expression in M1 macrophages; H-K, western blot analysis of the effect of GA on M2 marker protein expression in M2 macrophages; L-O, low cytometry validation of GA's effect on M1/M2 macrophage polarization status. CD86 positive indicates M1 macrophages. CD206 positive indicates M2 macrophages; P, schematic diagram of the co-culture system for HCC cells and M2 macrophages; Q-R, secretion levels of M2 macrophage-related cytokines (IL-10, TGF-β1) after GA treatment, detected by enzyme-linked immunosorbent assay; S-T, Proliferation of HCC cells detected by EdU staining (scale bar: 50 μm); U-V, invasion of HCC cells detected by Transwell assay (scale bar: 100 μm); W-X, migration of HCC cells detected by scratch assay (scale bar: 200 μm); Y-Z, apoptosis of HCC cells detected by flow cytometry (ns, $P > 0.05$, * $P < 0.05$, ** $P < 0.01$, *** $P < 0.001$ vs control).

4.5. Glycyrrhetinic Acid Induces Autophagy by Inhibiting the Activation of the TGF-β1/SMAD Pathway

To clarify whether the TGF-β1/SMAD pathway mediated GA-induced autophagy, a TGF-β1 activator (SRI-011381) was used for intervention. Combined treatment with SRI-011381 and 150 μM GA significantly reversed the inhibitory effect of GA on TGF-β1 expression and SMAD2/3 phosphorylation (Figure 6A-D). Regarding autophagy detection, SRI-011381 significantly reduced the number of GFP-LC3 and mRFP-LC3 fluorescent puncta in GA-treated cells, suggesting that autophagic flux was inhibited (Figure 6E-G). Moreover, SRI-011381 reversed the GA-induced increase in the LC3-II/LC3-I ratio and the expression levels of p62 and Beclin1 (Figure 6H-J). These results indicate that GA induces autophagy in HCC cells by inhibiting the activation of the TGF-β1/SMAD axis.

4.6. Glycyrrhetinic Acid Regulates the TGF-β1/SMAD Pathway to Induce Autophagy in Cancer Cells In Vivo and Inhibit Tumor Growth

Building on our in vitro evidence, we established a subcutaneous Hepa1-6 xenograft model to validate the anti-tumor efficacy of GA and its regulation of the TGF-β/SMAD/autophagy axis in vivo within a complex physiological environment. Western blot analysis revealed a substantial reduction in both TGF-β1 expression and SMAD2/3 phosphorylation within the tumor tissues following GA treatment (Figure 7A-D). Notably, the administration of SRI-011381 not only effectively reversed GA's inhibitory impact on the TGF-β1/SMAD axis but also abrogated the GA-induced upregulation of autophagy markers, including LC3-II/LC3-I, p62, and Beclin1 (Figure 7E-H). GA significantly suppressed tumor volume and mass, with the 50 mg/kg GA group showing a superior inhibitory effect

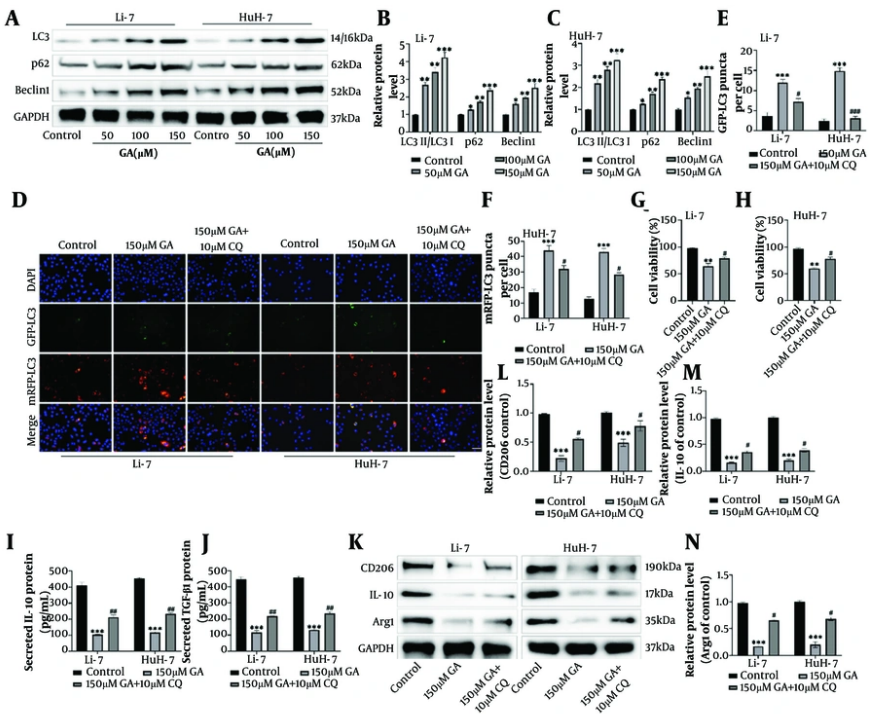

Figure 4. Glycyrrhetinic acid induces autophagy in HCC cells, thereby interfering with M2 polarization of TAMs. A-C, to investigate the effect of GA on autophagy, this study detected its impact on the expression of key autophagy marker proteins in HCC cells via Western blot; D-F, experimental groups: Control, 150 μM GA, and co-treatment with 150 μM GA and 10 μM chloroquine (CQ). The effect of GA on autophagic flux was observed by analyzing fluorescent puncta in HepG2 and SMMC-7721 cells transfected with mRFP-GFP-LC3B virus. Yellow puncta (colocalization of mRFP and GFP) represent autophagosomes not fused with lysosomes; orange-red puncta (mRFP signal only) represent autolysosomes fused with lysosomes (scale bar: 50 μm); G-H, viability of HCC cells detected by cell counting kit-8 assay; I-N, co-culture of HCC cells (control, 150 μM GA, 150 μM GA + 10 μM CQ) with M2 macrophages in a Transwell system to detect changes in the M2 macrophage phenotype; I-J, secretion levels of M2 macrophage-related cytokines IL-10 and TGF-β1 in culture supernatant detected by enzyme-linked immunosorbent assay; K-N, protein expression levels of M2 macrophage markers CD206, IL-10, and Arg1 detected by Western blot (* $P < 0.05$, ** $P < 0.01$, *** $P < 0.001$ vs control; # $P < 0.05$, ## $P < 0.01$ vs 150 μM GA).

compared to the 25 mg/kg GA group (Figure 7I-K). However, the combined use of SRI-011381 significantly reversed GA's inhibitory effect on tumor growth, leading to a notable increase in tumor volume and weight. Furthermore, GA treatment significantly reduced Ki67 expression in tumor tissues and markedly increased the number of terminal deoxynucleotidyl transferase dUTP nick end labeling-positive cells (Figure 7L-O), suggesting that GA inhibited tumor cell proliferation and promoted apoptosis in vivo. Conversely, SRI-011381 intervention reversed these GA-mediated effects. Collectively, these findings demonstrate that GA inhibits tumor growth in vivo by inducing autophagy through suppression of the TGF-β1/SMAD signaling pathway. Additionally, no pathological changes were detected in the liver and kidney tissues of mice from any group (Figure 7P), which indicates that GA exhibits no significant systemic toxicity at the administered doses.

4.7. Glycyrrhetinic Acid Inhibits M2 Macrophage Polarization in vivo by Regulating the TGF-β1/SMAD Pathway

To evaluate the impact of GA on the TME in vivo, we performed immunophenotypic analysis of single-cell suspensions from mouse tumor tissues. Flow cytometric results revealed that GA treatment led to a significant decrease in the proportions of TAMs (identified as F4/80+CD11b+ cells) and M2-polarized macrophages (CD206+) (Figure 8A-D). The combined use of SRI-011381 significantly reversed GA's inhibitory effect on M2 macrophage polarization. When BMDMs from each group of mice were co-cultured with Hepa1-6 cells, the levels of IL-10 and TGF-β1 in the co-culture supernatant of the GA-treated group were significantly lower compared to the Control group (Figure 8E-F), while the SRI-011381 combined treatment group restored the levels of these cytokines. GA treatment reduced the protein

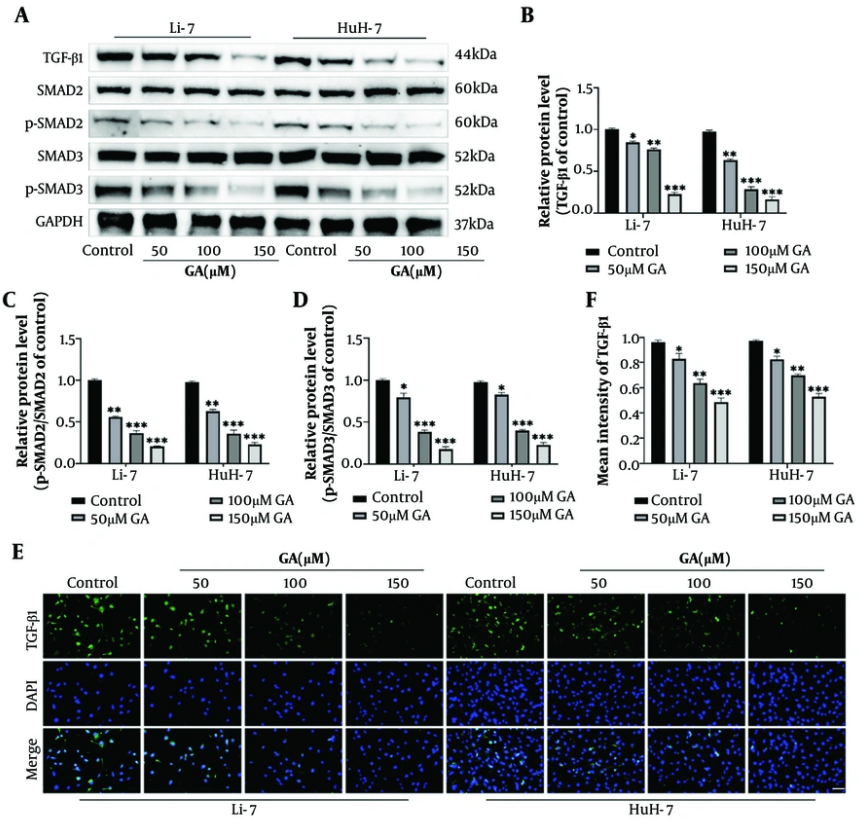

Figure 5. Glycyrrhetinic acid inhibits the TGF-β1/SMAD pathway. A-D, western blot analysis of the effect of GA treatment on the expression levels of key proteins in the TGF-β1/SMAD pathway in HCC cells; E-F, immunofluorescence staining validation of GA's effect on TGF-β1 protein expression in HCC cells (scale bar: 50 μm) (* $P < 0.05$, ** $P < 0.01$, *** $P < 0.001$ vs control).

expression of M2 markers in BMDMs (Figure 8G-J). A marked decrease in the percentage of CD206-positive BMDMs was also observed following GA treatment, indicating inhibition of M2 polarization (Figure 8K-L). This GA-induced alteration was successfully reversed when cells were co-treated with SRI-011381.

5. Discussion

The treatment of HCC remains a global focus and challenge in cancer research (29). Natural compounds have garnered widespread attention in anti-tumor drug development due to their multi-target properties and low toxicity (30). Our study demonstrated that GA directly inhibited HCC cell proliferation, migration, invasion, and induced apoptosis, which aligns with previous reports on the anti-cancer activity of GA and its derivatives in HCC (31, 32). However, the complexity of HCC lies in the highly immunosuppressive nature of its TME, particularly the M2-polarized TAMs, which play a central role in tumor progression (33). Our research delved into the mechanism of GA's action on the TME, revealing that GA significantly inhibited M2 macrophage polarization, reduced the secretion of pro-tumorigenic factors, and reversed the M2 macrophage-mediated promotion of HCC cell malignant phenotypes. This finding is highly consistent with recent therapeutic strategies targeting TAMs to overcome immune evasion (34). For instance, some studies have shown that traditional Chinese medicine extracts can effectively reprogram TAMs to an anti-tumor M1 phenotype by inhibiting TAM pathways (35). In vitro co-culture experiments confirmed that GA's inhibitory effect on M2 polarization was indirectly achieved through the regulation of HCC cells, rather than by directly acting on macrophages. Research indicates that the TGF-β1/SMAD axis is a critical driver of HCC progression, metastasis,

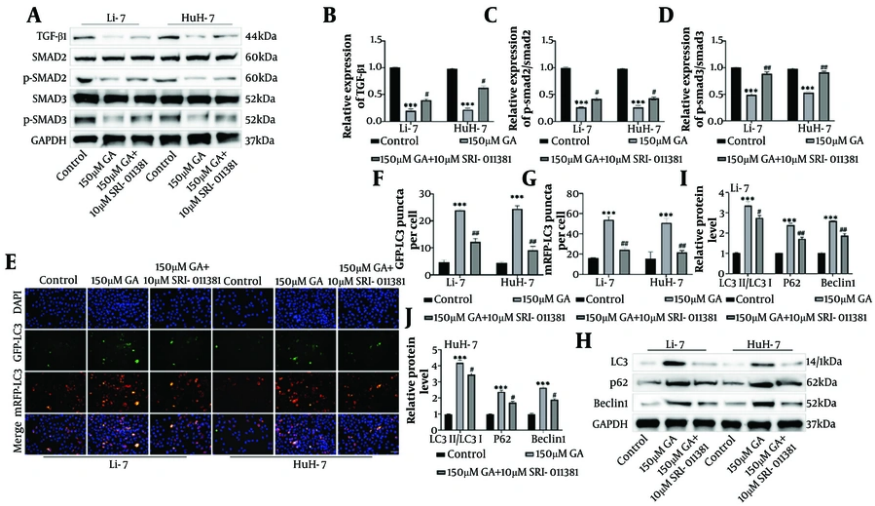

Figure 6. Glycyrrhetinic acid (GA) induces autophagy by inhibiting the activation of the TGF-β1/SMAD pathway. A-D, experimental groups: Control, 150 μM GA, 150 μM GA + 10 μM SRI-011381. Western blot analysis of the expression and phosphorylation levels of key proteins in the TGF-β1/SMAD signaling pathway in HCC cells; E-G, effect of SRI-011381 on GA-induced autophagic flux analyzed by fluorescent puncta using mRFP-GFP-LC3B viral transfection. Yellow puncta represent autophagosomes, and orange-red puncta represent autolysosomes (scale bar: 50 μm); H-J, the expression levels of autophagy marker proteins in cells from each group (*** $P < 0.001$ vs control; # $P < 0.05$ vs 150 μM GA).

and immunosuppression (36). In HCC, TGF-β1 signaling acts as a potent pro-tumorigenic factor by promoting epithelial-mesenchymal transition (EMT) and inducing the infiltration of immunosuppressive cells, such as M2 macrophages (37, 38). Our study found that GA dose-dependently inhibited TGF-β1 expression and SMAD2/3 phosphorylation in HCC cells, suggesting that GA directly interferes with this core pro-tumorigenic pathway. More importantly, we utilized the TGF-β1 signaling activator SRI-011381 for critical mechanistic validation. The addition of SRI-011381 not only restored the activation of the TGF-β1/SMAD pathway but also reversed GA's anti-tumor effects, including inhibition of tumor growth and M2 macrophage polarization. This strongly demonstrates that the TGF-β1/SMAD pathway is an upstream target through which GA exerts its anti-HCC and TME-regulating effects. This finding is consistent with previous research highlighting the critical role of TGF-β1 signaling in HCC immune evasion (39, 40). Autophagy exhibits a context-dependent duality in cancer, acting as either a pro-survival or pro-death mechanism (41). Notably, TGF-β signaling is a recognized suppressor of autophagy in various cellular systems (42). We observed that GA, by inhibiting the TGF-β1/SMAD pathway, promoted an increase in the LC3-II/LC3-I ratio and an upregulation of p62 and Beclin1 protein levels in HCC cells. During the initiation phase of autophagy, Beclin-1, as a core regulatory factor, forms a PI3K complex with Vps34 and others, initiating the formation of autophagosome precursors (43). In the elongation and maturation phases of autophagosomes, cytoplasmic LC3-I undergoes lipidation to form membrane-bound LC3-II, which specifically localizes to the autophagosomal membrane. Therefore, the LC3-II/LC3-I ratio is widely used as a key indicator to evaluate the extent of autophagosome formation (44). Simultaneously, p62, as a selective autophagy adaptor protein, on the one hand recognizes and binds ubiquitinated protein substrates, and on the other hand recruits these substrates to the expanding autophagosomal membrane through interaction with LC3-II, thereby mediating selective autophagy (45). This suggests that GA exerts its anti-tumor effects by promoting cellular autophagy through inhibition of the TGF-β1/SMAD pathway. Furthermore, our results indicated that the addition of the autophagy inhibitor CQ completely reversed the GA-mediated inhibition of M2 marker expression and IL-10/TGF-β1 secretion, confirming that GA-induced autophagy interferes with M2 macrophage polarization. We speculate that GA-induced autophagy alters the metabolic state or secretome of HCC cells, thereby releasing specific signaling molecules. These molecules, through a paracrine mechanism, act on macrophages, inhibiting their differentiation into the M2 phenotype. Such signaling molecules may include: (1) Autophagy-related

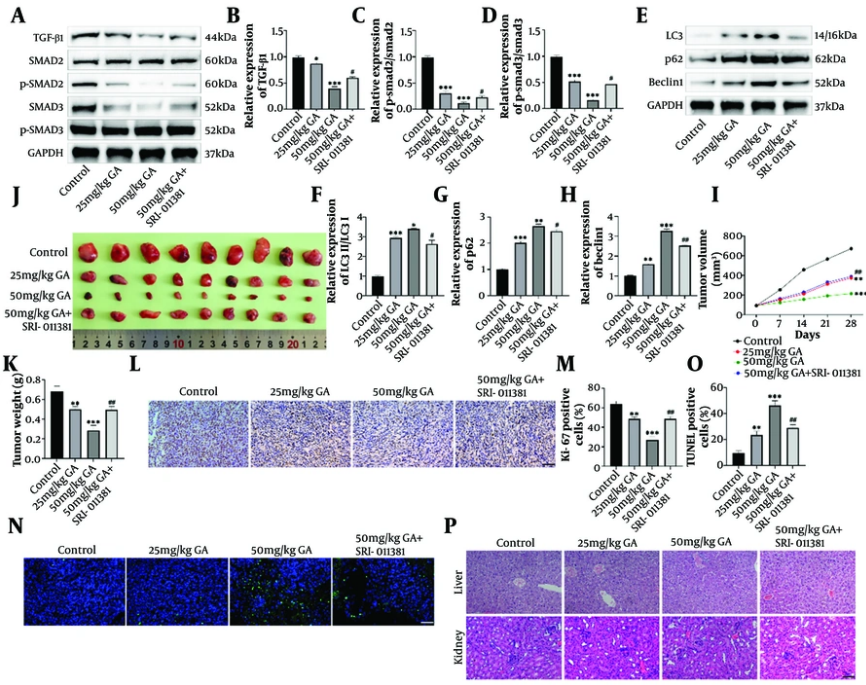

Figure 7. Glycyrrhetinic acid (GA) regulates the TGF-β1/SMAD pathway to induce autophagy in cancer cells in vivo and inhibit tumor growth. A-H, experimental groups: Control group, GA (25 mg/kg) group, GA (50 mg/kg) group, GA (50 mg/kg) + SRI-011381 (30 mg/kg) group (n = 9). Western blot analysis of the expression levels of key proteins in the TGF-β1/SMAD axis and autophagy marker proteins in mouse tumor tissues; I-K, evaluation of GA's inhibitory effect on tumor growth in mice; I, tumor volume change curve during treatment (days 0, 7, 14, 21, 28); J, representative photographs of tumors excised on day 28; K, tumor weight measured on day 28; L-M, expression levels of the proliferation marker Ki67 in mouse tumor tissues detected by immunohistochemistry staining; N-O, apoptosis levels of tumor cells detected by terminal deoxynucleotidyl transferase dUTP nick end labeling staining; P, pathological changes in mouse liver and kidney tissues observed by hematoxylin and eosin staining (scale bar: 50 μm) (* $P < 0.05$, ** $P < 0.01$, *** $P < 0.001$ vs control; # $P < 0.05$, ## $P < 0.01$ vs 50 mg/kg GA).

metabolites: Specific metabolic products generated during autophagy, such as amino acids or lipids, might be taken up by macrophages and interfere with the metabolic reprogramming required for their M2 polarization (46); (2) exosomes or extracellular vesicles: HCC cells undergoing autophagy might package specific microRNAs, proteins, or lipids into exosomes and release them. These exosomes, upon endocytosis by macrophages, could directly inhibit M2 polarization-related signaling pathways (e.g., STAT3 or HIF-1α) (47-49). The in vivo experimental results of this study have significant clinical translational implications. Glycyrrhetinic acid significantly inhibited the growth of Hepa1-6 xenograft tumors and ameliorated the immunosuppressive state within the TME (reduced M2 infiltration). More importantly, the TGF-β1 activator SRI-011381 reversed GA's anti-tumor and immunomodulatory effects in vivo, which not only confirms the criticality of GA's mechanism of action but also suggests that TGF-β1/SMAD pathway activation is a potential mechanism for HCC resistance to GA treatment. Glycyrrhetinic acid, as a natural, low-toxicity TGF-β1/SMAD inhibitor, possesses immense clinical potential. It could be used as a single agent for HCC treatment or in combination with existing immune checkpoint inhibitors (such as anti-PD-1/PD-L1 antibodies) (50). By inhibiting TGF-β1/SMAD and inducing autophagy, GA can effectively modulate the TME, reduce the proportion of M2 macrophages, and thereby enhance the efficacy of immune checkpoint inhibitors (51). Despite the significant progress made in this study, some limitations remain. Future research should delve deeper into precisely identifying the molecules released by GA-induced autophagic HCC cells that directly inhibit M2 polarization. Exploring the combined application of GA with other targeted drugs (e.g., those targeting VEGF or mTOR pathways) is also warranted to achieve more effective HCC treatment.

Conclusion This study confirmed that GA inhibits the malignant progression of HCC by suppressing the TGF-β1/SMAD axis, which in turn induces cellular autophagy

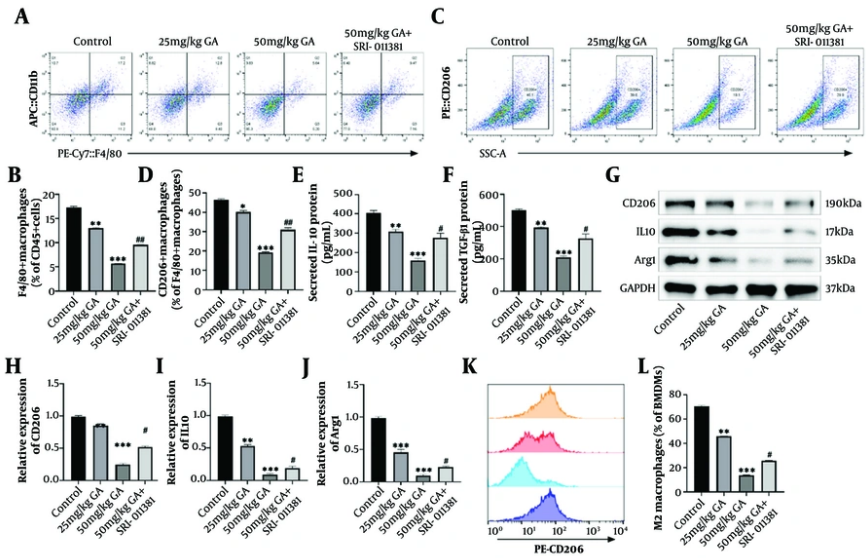

Figure 8. Glycyrrhetinic acid (GA) inhibits M2 macrophage polarization in vivo by regulating the TGF-β1/SMAD pathway. A-D, flow cytometry analysis of macrophage polarization in mouse tumor tissues; A-B, proportion of F4/80$^+$ total macrophages among tumor-infiltrating immune cells; C-D, proportion of CD206$^+$ M2 macrophages among F4/80$^+$ cells; E-F, in vitro co-culture system to validate the direct effect of GA on macrophage polarization. Mouse BMDMs were co-cultured with mouse HCC cells Hepa1-6 in a Transwell system. Enzyme-linked immunosorbent assay detection of secretion levels of M2 macrophage-related cytokines IL-10 and TGF-β1 in the co-culture supernatant; G-J, western blot analysis of the expression levels of M2 marker proteins (CD206, IL-10, Arg1) in BMDMs; K-L, proportion of CD206$^+$ cells in BMDMs within the co-culture system detected by flow cytometry (** $P < 0.01$, *** $P < 0.001$ vs control; # $P < 0.05$, ## $P < 0.01$ vs 50 mg/kg GA).

and inhibits M2 macrophage polarization. This work not only substantiates GA as a potential natural compound for HCC treatment but also uncovers a potential therapeutic target in HCC. Future research should focus on identifying the specific autophagy-related cargo molecules or metabolites released by GA-treated HCC cells that are involved in the inhibition of M2 macrophage polarization, which will provide new directions for developing combination therapy strategies for HCC.

Footnotes

AI Use Disclosure: The authors declare that no generative AI tools were used in the creation of this article.

Authors' Contribution: Youjin Wang and Huiyun Guan: Conceived and designed the research, conducted experiments, and analyzed data, drafted and revised the manuscript critically for important intellectual content; Huiyun Guan: Contributed to the acquisition, analysis, interpretation of data, and provided substantial intellectual input during the drafting and revision of the manuscript; Peibei Duan: Participated in the conception and design of the study and played a key role in data interpretation and manuscript preparation. All authors have read and approved the final version of the manuscript.

Conflict of Interests Statement: The authors declare no conflicts of interest.

Data Availability: The data that support the findings of this study are available from the corresponding author, upon reasonable request.

Ethical Approval: All animal experiments were approved by the Affiliated Hospital of Nanjing University of Chinese Medicine Ethics Committee (approval number: 2018NL-013-02).

Funding/Support: The authors declare no funding/support.

References

1. Sadri F, Rezaei Z. Noncoding RNAs: Key Modulators of the Hippo Pathway in Hepatocellular Carcinoma Progression. *J Cancer Biomolecul Therapeut.* 2025;**2**(1):73-88. https://doi.org/10.62382/jcbt.v2i1.36.

2. Singal AG, Kanwal F, Llovet JM. Global trends in hepatocellular carcinoma epidemiology: implications for screening, prevention and therapy. *Nat Rev Clin Oncol*. 2023;**20**(12):864-84. [PubMed ID: 37884736]. https://doi.org/10.1038/s41571-023-00825-3.
3. Singh SP, Madke T, Chand P. Global Epidemiology of Hepatocellular Carcinoma. *J Clin Exp Hepatol*. 2025;**15**(2):102446. [PubMed ID: 39659901]. [PubMed Central ID: PMC11626783]. https://doi.org/10.1016/j.jceh.2024.102446.
4. Ladd AD, Duarte S, Sahin I, Zarrinpar A. Mechanisms of drug resistance in HCC. *Hepatology*. 2024;**79**(4):926-40. [PubMed ID: 36680397]. https://doi.org/10.1097/HEP.0000000000000237.
5. Gao YX, Ning QQ, Yang PX, Guan YY, Liu PX, Liu ML, et al. Recent advances in recurrent hepatocellular carcinoma therapy. *World J Hepatol*. 2023;**15**(4):460-76. [PubMed ID: 37206651]. [PubMed Central ID: PMC10190692]. https://doi.org/10.4254/wjh.v15.i4.460.
6. de Visser KE, Joyce JA. The evolving tumor microenvironment: From cancer initiation to metastatic outgrowth. *Cancer Cell*. 2023;**41**(3):374-403. [PubMed ID: 36917948]. https://doi.org/10.1016/j.ccell.2023.02.016.
7. Sukei T, Palma E, Urbani L. Interplay between Cellular and Non-Cellular Components of the Tumour Microenvironment in Hepatocellular Carcinoma. *Cancers (Basel)*. 2021;**13**(21). [PubMed ID: 34771746]. [PubMed Central ID: PMC8583132]. https://doi.org/10.3390/cancers13215586.
8. Cheng K, Cai N, Zhu J, Yang X, Liang H, Zhang W. Tumor-associated macrophages in liver cancer: From mechanisms to therapy. *Cancer Commun (Lond)*. 2022;**42**(11):1112-40. [PubMed ID: 36069342]. [PubMed Central ID: PMC9648394]. https://doi.org/10.1002/cac2.12345.
9. Boutilier AJ, Elsawa SF. Macrophage Polarization States in the Tumor Microenvironment. *Int J Mol Sci*. 2021;**22**(13). [PubMed ID: 34209703]. [PubMed Central ID: PMC8268869]. https://doi.org/10.3390/ijms22136995.
10. Quaranta V, Ballaro C, Giannelli G. Macrophages Orchestrate the Liver Tumor Microenvironment. *Cancers (Basel)*. 2024;**16**(9). [PubMed ID: 38730724]. [PubMed Central ID: PMC11083142]. https://doi.org/10.3390/cancers16091772.
11. Chen S, Morine Y, Tokuda K, Yamada S, Saito Y, Nishi M, et al. Cancer-associated fibroblast-induced M2-polarized macrophages promote hepatocellular carcinoma progression via the plasminogen activator inhibitor-1 pathway. *Int J Oncol*. 2021;**59**(2). [PubMed ID: 34195849]. [PubMed Central ID: PMC8253588]. https://doi.org/10.3892/ijo.2021.5239.
12. Yu Z, Li Y, Li Y, Zhang J, Li M, Ji L, et al. Bufalin stimulates antitumor immune response by driving tumor-infiltrating macrophage toward M1 phenotype in hepatocellular carcinoma. *J Immunother Cancer*. 2022;**10**(5). [PubMed ID: 35618286]. [PubMed Central ID: PMC9125767]. https://doi.org/10.1136/jitc-2021-004297.
13. Zhang X, Yu C, Zhao S, Wang M, Shang L, Zhou J, et al. The role of tumor-associated macrophages in hepatocellular carcinoma progression: A narrative review. *Cancer Med*. 2023;**12**(24):22109-29. [PubMed ID: 38098217]. [PubMed Central ID: PMC10757104]. https://doi.org/10.1002/cam4.6717.
14. Kerneur C, Cano CE, Olive D. Major pathways involved in macrophage polarization in cancer. *Front Immunol*. 2022;**13**:1026954. [PubMed ID: 36325334]. [PubMed Central ID: PMC9618889]. https://doi.org/10.3389/fimmu.2022.1026954.
15. Vitaliti A, Reggio A, Palma A. Macrophages and autophagy: partners in crime. *FEBS J*. 2025;**292**(12):2957-72. [PubMed ID: 39439196]. [PubMed Central ID: PMC12176263]. https://doi.org/10.1111/febs.17305.
16. Wang Z, Wang G, Wang Y, Liu Q, Li H, Xie P, et al. Omp31 of Brucella Inhibits NF-kappaB p65 Signaling Pathway by Inducing Autophagy in BV-2 Microglia. *Neurochem Res*. 2021;**46**(12):3264-72. [PubMed ID: 34536195]. https://doi.org/10.1007/s11064-021-03429-4.
17. Gao Z, Li XG, Feng SR, Chen JF, Song K, Shi YH, et al. Autophagy suppression facilitates macrophage M2 polarization via increased instability of NF-kappaB pathway in hepatocellular carcinoma. *Int Immunopharmacol*. 2023;**123**:110685. [PubMed ID: 37494837]. https://doi.org/10.1016/j.intimp.2023.110685.
18. Ning J, Ye Y, Bu D, Zhao G, Song T, Liu P, et al. Imbalance of TGF-beta1/BMP-7 pathways induced by M2-polarized macrophages promotes hepatocellular carcinoma aggressiveness. *Mol Ther*. 2021;**29**(6):2067-87. [PubMed ID: 33601054]. [PubMed Central ID: PMC8178441]. https://doi.org/10.1016/j.ymthe.2021.02.016.
19. Gillson J, Abd El-Aziz YS, Leck LYW, Jansson PJ, Pavlakis N, Samra JS, et al. Autophagy: A Key Player in Pancreatic Cancer Progression and a Potential Drug Target. *Cancers (Basel)*. 2022;**14**(14). [PubMed ID: 35884592]. [PubMed Central ID: PMC9315706]. https://doi.org/10.3390/cancers14143528.
20. Zuo J, Meng T, Wang Y, Tang W. A Review of the Antiviral Activities of Glycyrrhizic Acid, Glycyrrhetinic Acid and Glycyrrhetinic Acid Monoglucuronide. *Pharmaceuticals (Basel)*. 2023;**16**(5). [PubMed ID: 37242424]. [PubMed Central ID: PMC10223068]. https://doi.org/10.3390/ph16050641.
21. Cheng Y, Zhong X, Nie X, Gu H, Wu X, Li R, et al. Glycyrrhetinic acid suppresses breast cancer metastasis by inhibiting M2-like macrophage polarization via activating JNK1/2 signaling. *Phytomedicine*. 2023;**114**:154757. [PubMed ID: 37011418]. https://doi.org/10.1016/j.phymed.2023.154757.
22. Fan Y, Dong W, Wang Y, Zhu S, Chai R, Xu Z, et al. Glycyrrhetinic acid regulates impaired macrophage autophagic flux in the treatment of non-alcoholic fatty liver disease. *Front Immunol*. 2022;**13**:959495. [PubMed ID: 35967372]. [PubMed Central ID: PMC9365971]. https://doi.org/10.3389/fimmu.2022.959495.
23. Wu S, Lu H, Wang W, Song L, Liu M, Cao Y, et al. Prevention of D-GalN/LPS-induced ALI by 18beta-glycyrrhetinic acid through PXR-mediated inhibition of autophagy degradation. *Cell Death Dis*. 2021;**12**(5):480. [PubMed ID: 33986260]. [PubMed Central ID: PMC8119493]. https://doi.org/10.1038/s41419-021-03768-8.
24. Huang Y, Tian C, Li Q, Xu Q. TET1 Knockdown Inhibits Porphyromonas gingivalis LPS/IFN-gamma-Induced M1 Macrophage Polarization through the NF-kappaB Pathway in THP-1 Cells. *Int J Mol Sci*. 2019;**20**(8). [PubMed ID: 31022963]. [PubMed Central ID: PMC6514734]. https://doi.org/10.3390/ijms20082023.
25. Genin M, Clement F, Fattaccioli A, Raes M, Michiels C. M1 and M2 macrophages derived from THP-1 cells differentially modulate the response of cancer cells to etoposide. *BMC Cancer*. 2015;**15**:577. [PubMed ID: 26253167]. [PubMed Central ID: PMC4545815]. https://doi.org/10.1186/s12885-015-1546-9.
26. Huang D, Xu M, Wang H, Zhao Y, Zhang Z, Yu M, et al. SIRPalpha blockade therapy potentiates immunotherapy by inhibiting PD-L1(+) myeloid cells in hepatocellular carcinoma. *Cell Death Dis*. 2025;**16**(1):451. [PubMed ID: 40523887]. [PubMed Central ID: PMC12170831]. https://doi.org/10.1038/s41419-025-07779-7.
27. Cai J, Song L, Zhang F, Wu S, Zhu G, Zhang P, et al. Targeting SRSF10 might inhibit M2 macrophage polarization and potentiate anti-PD-1 therapy in hepatocellular carcinoma. *Cancer Commun (Lond)*. 2024;**44**(11):1231-60. [PubMed ID: 39223929]. [PubMed Central ID: PMC11570766]. https://doi.org/10.1002/cac2.12607.
28. Gungor MZ, Uysal M, Senturk S. The Bright and the Dark Side of TGF-beta Signaling in Hepatocellular Carcinoma: Mechanisms, Dysregulation, and Therapeutic Implications. *Cancers (Basel)*. 2022;**14**(4). [PubMed ID: 35205692]. [PubMed Central ID: PMC8870127]. https://doi.org/10.3390/cancers14040940.
29. Brown ZJ, Tsilimigras DI, Ruff SM, Mohseni A, Kamel IR, Cloyd JM, et al. Management of Hepatocellular Carcinoma: A Review. *JAMA Surg*. 2023;**158**(4):410-20. [PubMed ID: 36790767]. https://doi.org/10.1001/jamasurg.2022.7989.

30. Zhou H, Zhang M, Cao H, Du X, Zhang X, Wang J, et al. Research Progress on the Synergistic Anti-Tumor Effect of Natural Anti-Tumor Components of Chinese Herbal Medicine Combined with Chemotherapy Drugs. *Pharmaceuticals (Basel)*. 2023;**16**(12). [PubMed ID: 38139860]. [PubMed Central ID: PMC10748242]. https://doi.org/10.3390/ph16121734.
31. Speciale A, Muscara C, Molonia MS, Cristani M, Cimino F, Saija A. Recent Advances in Glycyrrhetinic Acid-Functionalized Biomaterials for Liver Cancer-Targeting Therapy. *Molecules*. 2022;**27**(6). [PubMed ID: 35335138]. [PubMed Central ID: PMC8954912]. https://doi.org/10.3390/molecules27061775.
32. Stecanella LA, Bitencourt APR, Vaz GR, Quarta E, Silva Junior JOC, Rossi A. Glycyrrhizic Acid and Its Hydrolyzed Metabolite 18beta-Glycyrrhetinic Acid as Specific Ligands for Targeting Nanosystems in the Treatment of Liver Cancer. *Pharmaceutics*. 2021;**13**(11). [PubMed ID: 34834206]. [PubMed Central ID: PMC8621092]. https://doi.org/10.3390/pharmaceutics13111792.
33. Zhang Y, Han G, Gu J, Chen Z, Wu J. Role of tumor-associated macrophages in hepatocellular carcinoma: impact, mechanism, and therapy. *Front Immunol*. 2024;**15**:1429812. [PubMed ID: 39170620]. [PubMed Central ID: PMC11335564]. https://doi.org/10.3389/fimmu.2024.1429812.
34. Huang R, Kang T, Chen S. The role of tumor-associated macrophages in tumor immune evasion. *J Cancer Res Clin Oncol*. 2024;**150**(5):238. [PubMed ID: 38713256]. [PubMed Central ID: PMC11076352]. https://doi.org/10.1007/s00432-024-05777-4.
35. Zhang J, Gao J, Cui J, Wang Y, Jin Y, Zhang D, et al. Tumor-associated macrophages in tumor progression and the role of traditional Chinese medicine in regulating TAMs to enhance antitumor effects. *Front Immunol*. 2022;**13**:1026898. [PubMed ID: 36311793]. [PubMed Central ID: PMC9611775]. https://doi.org/10.3389/fimmu.2022.1026898.
36. Xin X, Cheng X, Zeng F, Xu Q, Hou L. The Role of TGF-beta/SMAD Signaling in Hepatocellular Carcinoma: from Mechanism to Therapy and Prognosis. *Int J Biol Sci*. 2024;**20**(4):1436-51. [PubMed ID: 38385079]. [PubMed Central ID: PMC10878151]. https://doi.org/10.7150/ijbs.89568.
37. Soukupova J, Malfettone A, Bertran E, Hernandez-Alvarez MI, Penuelas-Haro I, Dituri F, et al. Epithelial-Mesenchymal Transition (EMT) Induced by TGF-beta in Hepatocellular Carcinoma Cells Reprograms Lipid Metabolism. *Int J Mol Sci*. 2021;**22**(11). [PubMed ID: 34073989]. [PubMed Central ID: PMC8197297]. https://doi.org/10.3390/ijms22115543.
38. Fu X, Pang M, Wang Z, Wang H. Macrophage Polarization in the Tumor Microenvironment of Hepatocellular Carcinoma: From Mechanistic Insights to Translational Therapies. *Cancer Control*. 2025;**32**:10732748251406700. [PubMed ID: 41403016]. [PubMed Central ID: PMC12709032]. https://doi.org/10.1177/10732748251406674.
39. Jin X, Zhang S, Wang N, Guan L, Shao C, Lin Y, et al. High Expression of TGF-beta1 Contributes to Hepatocellular Carcinoma Prognosis via Regulating Tumor Immunity. *Front Oncol*. 2022;**12**:861601. [PubMed ID: 35547872]. [PubMed Central ID: PMC9082360]. https://doi.org/10.3389/fonc.2022.861601.
40. Bao S, Jiang X, Jin S, Tu P, Lu J. TGF-beta1 Induces Immune Escape by Enhancing PD-1 and CTLA-4 Expression on T Lymphocytes in Hepatocellular Carcinoma. *Front Oncol*. 2021;**11**:694145. [PubMed ID: 34249750]. [PubMed Central ID: PMC8270637]. https://doi.org/10.3389/fonc.2021.694145.
41. Liu S, Yao S, Yang H, Liu S, Wang Y. Autophagy: Regulator of cell death. *Cell Death Dis*. 2023;**14**(10):648. [PubMed ID: 37794028]. [PubMed Central ID: PMC10551038]. https://doi.org/10.1038/s41419-023-06154-8.
42. Zhang J, Jiang N, Ping J, Xu L. TGF-beta1-induced autophagy activates hepatic stellate cells via the ERK and JNK signaling pathways. *Int J Mol Med*. 2021;**47**(1):256-66. [PubMed ID: 33236148]. [PubMed Central ID: PMC7723502]. https://doi.org/10.3892/ijmm.2020.4778.
43. Guo R, Liu J, Min X, Zeng W, Shan B, Zhang M, et al. Reduction of DHHC5-mediated beclin 1 S-palmitoylation underlies autophagy decline in aging. *Nat Struct Mol Biol*. 2024;**31**(2):232-45. [PubMed ID: 38177673]. https://doi.org/10.1038/s41594-023-01163-9.
44. Sun B, Ma J, Te L, Zuo X, Liu J, Li Y, et al. Zinc-Deficient Diet Causes Imbalance in Zinc Homeostasis and Impaired Autophagy and Impairs Semen Quality in Mice. *Biol Trace Elem Res*. 2023;**201**(5):2396-406. [PubMed ID: 35713811]. https://doi.org/10.1007/s12011-022-03324-1.
45. Li W, He P, Huang Y, Li YF, Lu J, Li M, et al. Selective autophagy of intracellular organelles: recent research advances. *Theranostics*. 2021;**11**(1):222-56. [PubMed ID: 33391472]. [PubMed Central ID: PMC7681076]. https://doi.org/10.7150/thno.49860.
46. Shiau DJ, Kuo WT, Davuluri GVN, Shieh CC, Tsai PJ, Chen CC, et al. Hepatocellular carcinoma-derived high mobility group box 1 triggers M2 macrophage polarization via a TLR2/NOX2/autophagy axis. *Sci Rep*. 2020;**10**(1):13582. [PubMed ID: 32788720]. [PubMed Central ID: PMC7423894]. https://doi.org/10.1038/s41598-020-70137-4.
47. Xu Y, Xu L, Chen Q, Zou C, Huang J, Zhang L. Crosstalk between exosomes and tumor-associated macrophages in hepatocellular carcinoma: implication for cancer progression and therapy. *Front Immunol*. 2025;**16**:1512480. [PubMed ID: 40264760]. [PubMed Central ID: PMC12011854]. https://doi.org/10.3389/fimmu.2025.1512480.
48. Li D, Zhang T, Guo Y, Bi C, Liu M, Wang G. Biological impact and therapeutic implication of tumor-associated macrophages in hepatocellular carcinoma. *Cell Death Dis*. 2024;**15**(7):498. [PubMed ID: 38997297]. [PubMed Central ID: PMC11245522]. https://doi.org/10.1038/s41419-024-06888-z.
49. Wei Q, Liu G, Huang Z, Huang Y, Huang L, Huang Z, et al. LncRNA MEG3 Inhibits Tumor Progression by Modulating Macrophage Phenotypic Polarization via miR-145-5p/DAB2 Axis in Hepatocellular Carcinoma. *J Hepatocell Carcinoma*. 2023;**10**:1019-35. [PubMed ID: 37435155]. [PubMed Central ID: PMC10329916]. https://doi.org/10.2147/JHC.S408800.
50. Qiu X, Huang R, Xie J, Luo S, Cheng X, Cui J, et al. Recent Advances in the Therapeutic Effects and Molecular Mechanisms of Baicalin. *Biology (Basel)*. 2025;**14**(6). [PubMed ID: 40563888]. [PubMed Central ID: PMC12190052]. https://doi.org/10.3390/biology14060637.
51. Goyal H, Kaur J. Long non-coding RNAs and autophagy: dual drivers of Hepatocellular carcinoma progression. *Cell Death Discov*. 2025;**11**(1):376. [PubMed ID: 40789840]. [PubMed Central ID: PMC12339970]. https://doi.org/10.1038/s41420-025-02667-7.